Research Article

iMedPub Journals
www.imedpub.com

Health Science Journal
ISSN 1791-809X

2021
Vol. 15 No. 5: 834

The Therapeutic Possibility of EBV-Positive Nasopharyngeal Carcinoma through Targeting Somatostatin Receptors

Jinlei Ye[1], Shilei Wang[1], Shuo Liu[2], Ying Chen[1], Songhai Shen[1], Qiping Zheng[1], Zhilei Cui[3] and Lichun Sun[1,4]*

1 Shenzhen Academy of Peptide Targeting Technology at Pingshan and Shenzhen Tyercan Bio-Pharm Co., Ltd, Guangdong, China

2 Sino-US Innovative Bio-Medical Center and Hunan Beautide Pharmaceuticals, Xiangtan, Hunan, China

3 Department of Respiratory Medicine, Xin Hua Hospital Affiliated to Shanghai Jiao Tong University School of Medicine, Shanghai, China

4 Peptide Research Laboratories, Department of Medicine, Tulane University Health Sciences Center, New Orleans, LA 70112, USA

***Corresponding author:**
Lichun Sun

Tel: 504-988-1179

peptide612@gmail.com; lsun@tulane.edu

Peptide Research Laboratories, Department of Medicine, Tulane University Health Sciences Center, New Orleans, LA 70112, USA.

Citation: Ye J, Wang S, Liu S, Chen Y, Shen S, et al. (2021) The Therapeutic Possibility of EBV-Positive Nasopharyngeal Carcinoma through Targeting Somatostatin Receptors. Health Sci J. 15 No. 5: 834.

Abstract

Nasopharyngeal carcinoma (NPC) is a complex epithelial malignancy caused by both internal and environmental factors. Among them, Epstein–Barr virus (EBV) is a definitive etiological factor. The current therapeutic regimen for NPC is far from ideal and recurrence is commonly seen in patients after conventional radio and/or chemotherapy. We have thereby set out to develop new treatments for this deadly disease. Having analyzed a number of nasopharyngeal tissue and cell samples, we found that the level of somatostatin receptors (SSTRs) was positively correlated with EBV infection. Further, SSTR2 is the dominant SSTR isoform expressed in the EBV-positive (EBV (+)) NPC cells, a potential target for precise delivery of therapeutic agents. Cytotoxic effects of small molecule drugs including ansamitocin P-3 (AP-3), camptothecin and colchicine were subsequently evaluated in NPC cells. We found that AP-3 exhibits its strong anti-NPC activities with the IC50 values being 0.07 nM in EBV (+) NPC C666-1 cells and 0.09 nM in EBV (-) NPC CNE2 cells. In the xenograft animal model, AP-3 further shows inhibitory effects on NPC growth. These findings indicated that AP-3's activity is not related to EBV in NPC cells. Thus, we proposed that SSTR2-specific delivery of AP-3 via linking AP-3 to somatostatin is likely a viable option to treat the EBV (+) NPC patients.

Keywords: Nasopharyngeal carcinoma (NPC); Epstein–Barr virus (EBV); Ansamitocin P-3 (AP-3); Somatostatin receptors; Cell proliferation; Tumor growth

Received with Revision May 02, 2021, **Accepted:** May 17, 2021, **Published:** May 21, 2021

Introduction

Nasopharyngeal carcinoma (NPC) is an epithelial cancer originates from the nasopharynx epithelium. NPC shows a unique geographical distribution and is prevalent in Southern China, Southeast Asia and North Africa [1-3]. NPC seems mainly affecting Asian in the endemic region, people living in nearby Asian countries such as Korea and Japan are rarely affected [2-4]. Although the etiology of NPC is still largely unclear, the current evidence indicate that the high incidence in the endemic regions is strongly associated with the consumption of local traditional food including smoked meats, salted foods and preserved foods. NPC is also associated with several other etiological factors such as chemical carcinogens, toxic pollutants, genetic susceptibility and Epstein–Barr virus (EBV) infection [5-7].

Based on the tumor differentiation profiles, NPC can be classified into three subtypes (Type I, II and III) [1]. Type I NPC is categorized to the differentiated and keratinizing squamous cell carcinoma. The tumor cells are well differentiated with abundant keratin production. Type II NPC is the differentiated and non-keratinizing squamous cell carcinoma. Type III NPC is undifferentiated and non-keratinizingsquamous cell carcinoma. More than 95% of NPC cases in Southern China belong to type II and III or non-keratinizing carcinomas. Both types II and III NPC are highly associated with EBV infection, while Type I is not [1,2,4] Although NPC cells are commonly infected by EBV, normal nasopharyngeal epithelial cells don't carry EBV genome. Thus, EBV encoded gene products and associated cellular signaling molecules may serve as unique targets for precise management of EBV (+) NPC [6].

Lacking unique symptoms, NPC are not easily diagnosed at the early stage [4]. Most patients are diagnosed at the late stage and succumb to this deadly disease. In addition to surgery, NPC patients are routinely treated with radio and chemotherapy because NPC is highly sensitive to radiation and chemo-drugs [8]. Recently, new EBV-based immunotherapy and gene therapy were also implemented in the NPC management [7-9]. In this study, we discovered a strong correlation of EBV infection and the level of somatostatin receptors (SSTRs), a large family of G protein-coupled receptors (GPCRs). SSTRs highly expressed in EBV-positive NPC cells/tissues, but not in EBV-negative cells. Our finding indicates that SSTR-targeting drugs is likely a good candidate for the treatment of EBV-positive NPCs.

Materials and Methods

Compounds/Chemicals

The compounds ansamitocin P-3 (AP-3), camptothecin and colchicine were purchased from MCE (MedChemExpress, NJ, USA), with > 98% purity.

Cell culture

The EBV-positive NPC (C666-1) and EBV-negative NPC (CNE2) cell lines were purchased from the Beijing Nightingale Consultation of Culture (Beijing, China). Both NPC C666-1 and CNE2 cells were maintained in RPMI 1640 medium, supplemented with 10% fetal bovine serum (FBS) and 1% penicilin/streptomycin. All cells were cultured in a humidified incubator (Thermo Fisher Scientific, Waltham, MA, USA) at 37°C in a 5% CO_2 atmosphere.

Analysis of RNA-sequencing datasets

Raw RNA-sequencing data sets of primary nasopharyngeal epithelial cells, NPC cell lines and primary cancer tissues were obtained from the Gene Expression Omnibus under accession number GSE54174 as well as the NCBI Sequence Read Archive (SRP049967). NP460 is an EBV (-) immortalized nasopharyngeal cell line. HK1 is an EBV (-) well differentiated NPC cell line. C666-1 is an EBV (+) undifferentiated NPC cell line as said above. X666-1 is an EBV (+) NPC xenograft. All three primary NPC tissues (SRR1654790, SRR1654791 and SRR1654793)were infected with EBV. The transcriptome data were first analyzed by our RNA CoMPASS pipeline (REF1) to detect EBV transcripts and then analyzed by the RSEM algorithm for quantification of human gene expression as previously described (REF2) to calculate the relative levels of SSTR RNA present in these cells [6,10].

Quantitative polymerase chain reaction (qPCR) assay

Total RNAs were extracted using the total RNA Kit (OMEGA). RNAs were reverse transcribed into complementary DNA (cDNA). Following cDNA synthesis, qPCR reactions were performed in triplicate for each of the individual samples using the SYBR Green (Genecopoeia, USA) detection method by a Step One PCR machine (Bio-Rad). The primers used for detecting viral and cellular genes (LMP1, LMP2, EBNA3A, EBNA3C, BART, BHRF1, EBNA1, EBER, SSTR1, SSTR2, SSTR3, SSTR4 and SSTR-5) [5,11] are shown in **Table 1.** Expression was normalized with the internal control β-actin purchased from Genecopoeia (USA). The relative expression was calculated through the $2^{-\Delta\Delta Ct}$ method.

Table 1 The sequences of primers designed for qPCR analysis of EBV relative genes and SSTRs.

Primer		5'---3'
SSTR1	F	GGAGCCGGTTGACTATTACG
	R	CAGGTTCTCAGGTTGGAAGTC
SSTR2	F	GCCGTACTATGACCTGACAAG
	R	TCTTCATCTTGGCATAGCGG
SSTR3	F	CCCTTCAGTCACCAACGTCT
	R	TGGTGAACTGGTTGATGCCA
SSTR4	F	GCATGGTCGCTATCCAGTG
	R	GCGAAGGATCACGAAGATGAC
SSTR5	F	TGTTTGCGGGATGTTGGCT
	R	CTGTTGGCGTAGGAGAGGA
LMP1	F	CCACTTGGAGCCCTTTGTMTACTC
	R	TGCCTGTCCGTGCAAATTC
LMP2A	F	TGACTCATCTCAACACATATACGAAGAA
	R	GGTAGGGCGCAACAATTACAG
EBNA1	F	CAGTAGACCTGGGAGCAGATTCA
	R	TGGCCCCTCGTCAGACAT
EBNA2	F	GCGCCAATCTGTCTACATAGAAGA
	R	AGTGCTGGGTTACTGGCTAAGC
EBER	F	AGGACCTACGCTGCCCTAGAG
	R	AACCACAGACACCGTCCTCAC
BART8	F	GGGTCACAATCTATGGGGT
	R	CAGTGCGTGTCGTGGAGT
BART14	F	TACCCTACGCTGCCG
	R	TGCGTGTCGTGGAGTC
BHRF1	F	GGAGATACTGTTAGCCCTG
	R	GTGTGTTATAAATCTGTTCCAAG

Cell viability assay

Cell viability assay was conducted using the Cell Counting Kit-8 (CCK-8; Dojindo, Kumamoto, Japan) following the manufacturer's protocol. Briefly, cells were seeded in 96-well cell culture plates at a cell density of 8×10^3 cells per well, with different concentrations of compounds added to each well, respectively. The content in wells were mixed well. The plates were incubated at 37°C for 72 h. Then 10 μL of CCK-8 solution was added and the plates were incubated for another 1-4 h. The OD values were measured at 450 nm by a microplate reader (BioTek, USA).

Cell apoptosis analysis

C666-1 and CNE2 cells (2×10^5 cells per well) were seeded into 6-well plates, and treated with AP-3 for 48 h. Cell apoptosis assay was then performed according to the manufacturer's instruction. Briefly, the treated cells were collected by centrifugation at 1500 rpm for 5 min. After washed twice with PBS, the cells were suspended in 100 μL binding buffer and were incubated with 5 μL FITC-AV and 5 μL PI for 15 minutes in the dark place at room temperature. Subsequently, additional 400 μL binding buffer was added and analysis was performed by a Cyto FLEX flow cytometer.

Cell cycle analysis

C666-1 and CNE2 cells (2×10^5 cells /well) were cultured in 6-well

plates and treated with AP-3 (0, 0.2 and 0.4 nM for C666-1; 0, 0.1 and 0.2 nM for CNE2) for 24 h. After digested with 0.25% non-EDTA trypsin, the cell suspension was collected and centrifuged at 1500 rpm for 5 min. The cells were harvested, washed twice with PBS, fixed with 70% cold ethanol at -20°C for 24 h. After centrifuged at 4000 rpm for 2 min, the supernatants were removed, cells were suspended in 500 µL PBS with 0.25% Triton-X 100 and incubated for 15 min on ice. After centrifuged, the supernatant was discarded, each tube was added with 500 µL PBS containing 10 µg/mL RNase A and 20 µg/mL PI, and incubated in the dark place at room temperature for 30 minutes. Finally, the cell samples were placed in Falcon tubes and analyzed by a CytoFLEX flow cytometry.

Xenograft mouse model

Female BALB/c nude mice aged at 4-6 week-old were purchased and reared in the laboratory animal facility for one week to adapt to the new environment. A total of 5 × 10^6 C666-1 cells (200 µl) were inoculated into the right flank of each mouse bysubcutaneous injection. While the tumor sizes reached 100-300 mm^3 (Tumor volume = 0.5 × Length × $Width^2$), tumor-carrying mice were given by tail vein injection with 100 µl of the tested compound AP-3 at the dose of 0.3 mg/kg in the experimental group, with 100 µl normal saline containing 10% alcohol used in the control group. Mice were treated once a week for four weeks. Tumor volumes were measured and mouse bodies were weighed twice a week since the first administration.

Results

SSTR2 is a potential drug target for EBV-positive NPCs

Previous studies report such relationship using traditional method [12]. We use more accurate RNA-seq analysis and confirm this phenomenon. We first conducted RNA-seq analysis to interrogate the level of SSTRs in nasopharyngeal cells/tissues. SSTRs were not detectable in EBV (-) immortalized nasopharyngeal NP460 cells, or in EBV (-) well-differentiated NPC cells (HK1). However, SSTRs were abundantly expressed in EBV (+) NPC C666-1 cells, EBV (+) NPC X666-1 xenograft and primary NPC tissues (SRR1654790, SRR1654791 and SRR1654793) **(Figure 1).**

To validate this observation, we did qRT-PCR assay of both EBV (+) NPC C666-1 cells and EBV (-) NPC CNE2 cells. Our data confirmed the presence of EBV gene products (EBER, EBNA1, LMP1/2A, BHRF1) in EBV (+) NPC C666-1 cells **(Figure 2),** but not in EBV (-) NPC CNE2 cells. Among SSTR isoforms, high level of SSTR2 was also found in EBV (+) NPC C666-1 cells **(Figure 3).** Our findings support the notion that in the context of NPC, SSTR2 is likely a surrogate marker for EBV infection and provide a potential therapeutic strategy in the treatment of EBV (+) NPC patients via designing a SSTR2-targeting drug.

SSTR2 is an isoform of SSTR family, a key component of GPCRs. High level of SSTR has been reported in several cancers such as lung cancers, breast cancer and neuroblastoma. Somatostatin is the short peptide ligand of SSTRs. A modified somatostatin analog or an anti-SSTR2 monoclonal antibody (mAb) could preferentially

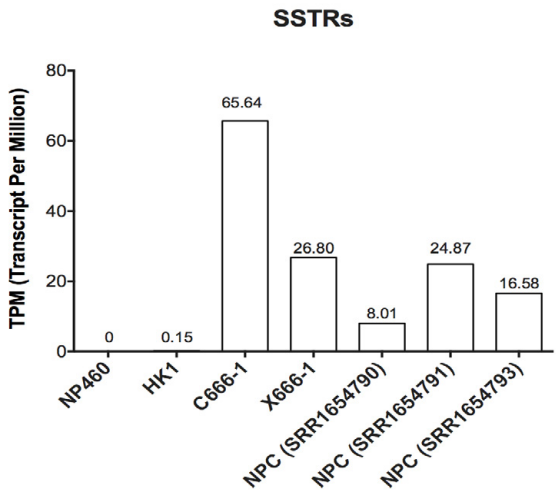

Figure 1 RNA-seq analysis. Raw RNA-sequencing data sets were gotten from the Gene Expression Omnibus under accession number GSE54174 and the NCBI Sequence Read Archive SRP049967. The transcriptome data were analyzed by RNA CoMPASS pipeline (REF1) to detect EBV transcripts and then analyzed by the RSEM algorithm for quantification of human gene expression to calculate the relative levels of SSTR RNA. NP460 is an EBV (-) immortalized nasopharyngeal cell line. HK1 is an EBV (-) well differentiated NPC cell line. C666-1 is an EBV (+) undifferentiated NPC cell line. X666-1 is an EBV (+) NPC xenograft. SRR1654790, SRR1654791 and SRR1654793 are the three primary NPC tissues.

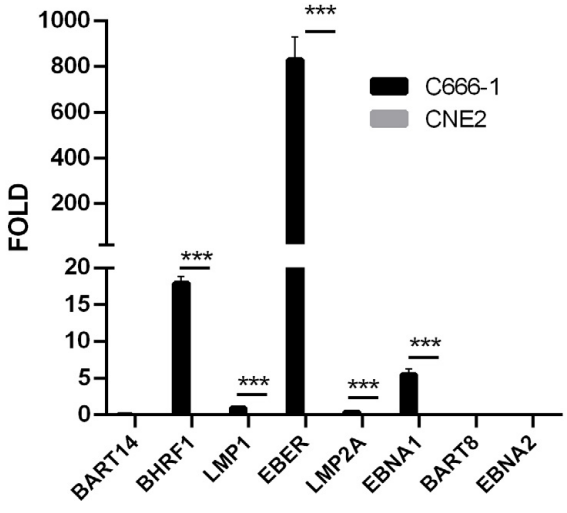

Figure 2 qPCR analysis showed the expression of EBV-associated genes in both EBV (+) NPC C666-1 and EBV (-) NPC CNE2 cells, including BART8, BART14, BHRF1, LMP1, LMP2A, EBER, EBNA1 and EBNA2. EBER wa abundantly expressed in EBV (+) NPC C666-1 cells, with BHRF1, EBNA1, LMP1 and LMP2A less and the other undetectable. All investigated genes were not detected in EBV (-) NPC CNE2 cells.

target SSTR2. Thus, the strategy via the interaction of ligand and receptor could be used to deliver drug to NPC target sites. We proposed to conjugate a small molecule cytotoxic agent with

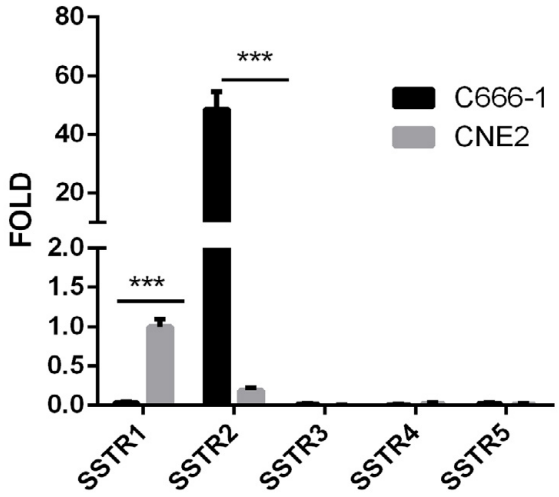

Figure 3 qPCR analysis showed the expressional profiles of somatostatin receptors (SSTRs) in both EBV (+) NPC C666-1 and EBV (-) NPC CNE2 cells. SSTR2 was highly expressed in EBV (+) NPC C666-1 cells, predicting SSTR2 may be a potential target in EBV (+) NPCs.

the ligand somatostatin or anti-SSTRs mAb. These new drug conjugates could most likely deliver drug to SSTR2-specific EBV (+) NPCs.

The suppressive effects of the tested compounds on cell proliferation

Three cytotoxic compounds **ansamitocin** P-3 **(AP-3),** camptothecin and colchicine were tested for NPC treatments. First, we did cell proliferation assay to examine their anti-proliferative activities. As shown in **Figure 4**, all three compounds inhibited the growth of both EBV (+) NPC C666-1 and EBV (-) NPC CNE2 cells. The IC_{50} values of **AP-3,** camptothecin and colchicine in treating CNE2 cells were 0.09 nM, 81.8 nM and 14.1 nM, respectively. The IC_{50} values in treating C666-1 cells are 0.07 nM for AP-3, 51.6 nM for camptothecin and 3.4 nM for colchicine. Their cytotoxic activities were not affected by the EBV positivity. Notably, AP-3 has the highest killing efficacy compared to the ones of camptothecin and colchicine, with one hundred times stronger than the other two, which makes AP-3 a good candidate for drug conjugate.

The effects of the compound AP-3 on cell apoptosis and cell cycle progression

We next conducted the flow cytometry assay to further examine the effects of AP-3 on cell apoptosis and cell cycle progression. As shown in **Table 2** and **Figure 5**, AP-3 induced apoptosis of C666-1 cells in a dose-dependent manner, with apoptosis rates of 26.19 ± 4.57% (0.4 nM) and 33.61 ± 2.88% (0.8 nM), respectively. The apoptosis rates in treated CNE2 cells are from 14.56 ± 3.90% (control) to 20.88 ± 0.81% (0.1 nM) and 38.20 ± 8.63% (0.2 nM). Meanwhile, AP-3 also effectively induced G2/M growth arrest in both NPC C666-1 and CNE2 cells in a dose-dependent manner. AP-3-induced G2/M growth arrest in C666-1 cells is from 26.90 ± 3.53% (control) to 51.76 ± 9.84% (0.4 nM) and 66.20 ± 5.60% (0.8 nM), respectively. Meanwhile, the AP-3-treated CNE2 cells

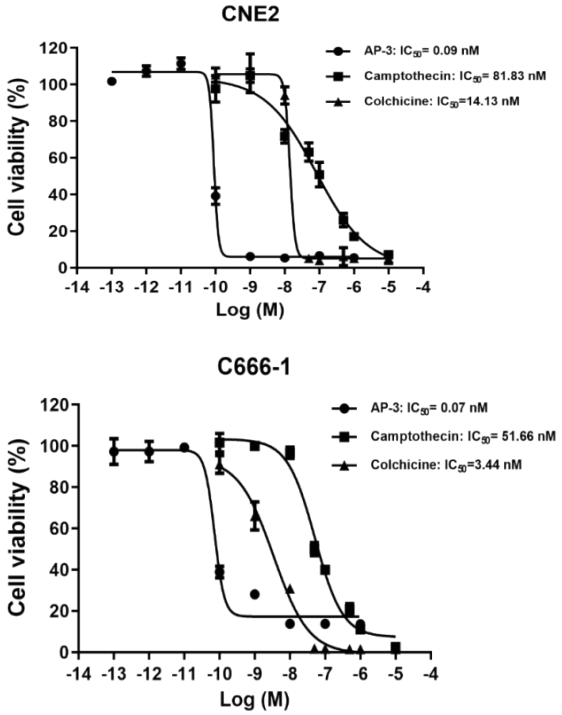

Figure 4 The suppressive effects of the cytotoxic compounds AP-3, camptothecin and colchicine in both EBV (+) NPC C666-1 and EBV (-) NPC CNE2 cells. AP-3 displayed over hundreds of more activity than the other two, with IC_{50} values being 0.09 nM in CNE2 and 0.07 nM in C666-1 cells, respectively.

Table 2 Ansamitocin P3 (AP-3) induced EBV (-) CNE2 and EBV (+) C666-1 cell apoptosis in a dose-dependent manner.

Cell	Concentration of AP-3 (nM)	Apoptosis (%)		
		Early stage	Late stage	Total
C666-1	0	5.72±2.01	13.23±1.46	18.95±0.87
	0.4	15.17±5.00	10.99±1.73	26.19±4.57
	0.8	24.10±2.10	9.51±1.02	33.61±2.88
CNE2	0	3.16±0.79	11.40±3.11	14.56±3.90
	0.1	7.93±1.53	12.95±2.33	20.88±0.81
	0.2	16.15±4.03	22.05±12.66	38.20±8.63

showed a growth arrest from 20.41 ± 0.43% (control) to 47.13 ± 9.50 % (0.1 nM) and 72.37 ± 2.18% (0.2 nM) **(Table 3 and Figure 6).**

The suppression of compound AP-3 on tumor growth *in vivo*

The *in vitro* assays showed a potent cytotoxic effect of AP-3 on EBV (+) and EBV (-) NPC cells. We next investigated the anti-tumor efficacy of AP-3 in xenograft mouse model. The EBV (+) C666-1 cells were injected under skin of nude mice. Mice carrying tumors with the average volume size being about 100-300 mm^3 were separated into two groups (n=8), and AP-3 at a dose of 0.3 mg/kg was administered by tail vein injection. As shown in Figure 5, tumor volumes in control group increased from 135.30 ± 18.58 mm^3 (Day 0) to 2611.35 ± 507.09 mm^3 (Day 30), with an increased rate of 1830.4%. Tumor volumes in AP-3 group rose from 138.11

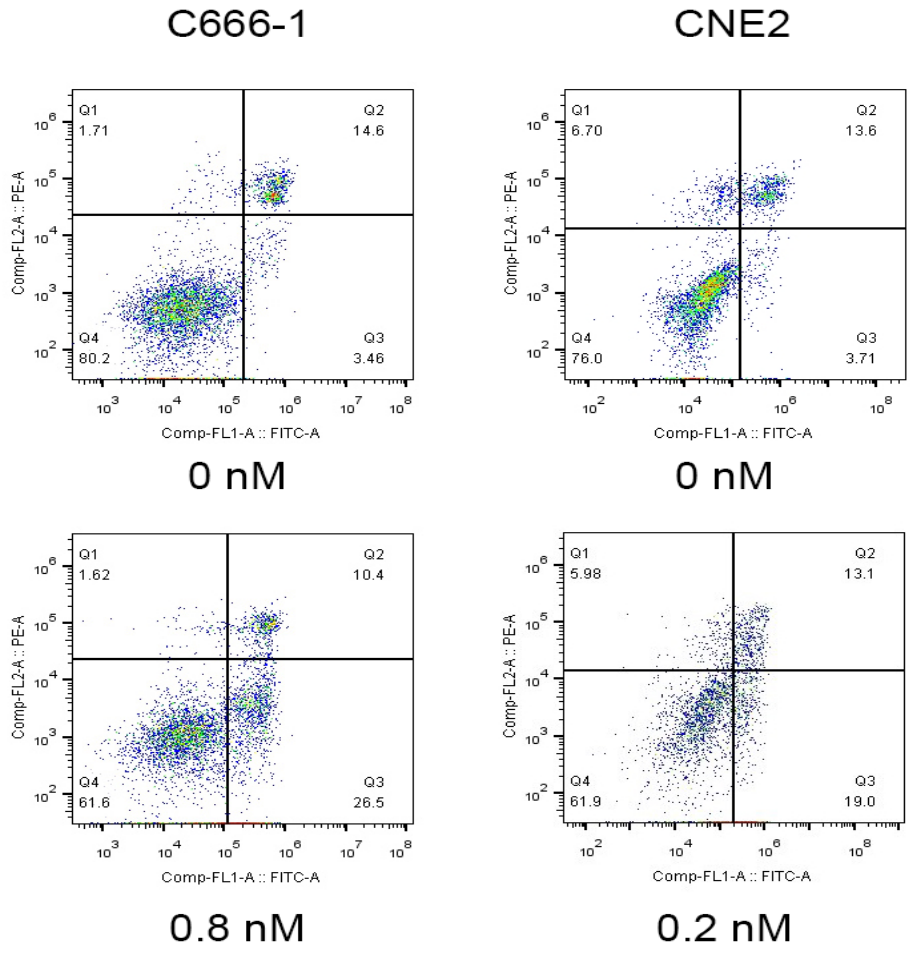

Figure 5 The compound AP-3 induced cell apoptosis in EBV (+) NPC C666-1 and EBV (-) NPC CNE2 cells. Cells were treated with AP-3 for 48 hours. Q1, Q2, Q3, and Q4 represent dead cells, late apoptosis, early apoptosis and alive cells, respectively.

Table 3 Ansamitocin P3 (AP-3) induced cell cycle arrest at G2/M phases in EBV (-) CNE2 and EBV (+) C666-1 cells and in a dose-dependent manner.

Cell	Concentration of AP-3 (nM)	Phases (%)		
		G0/G1	S	G2/M
C666-1	0	51.89±1.97	21.22±1.64	26.90±3.53
	0.4	25.95±10.02	22.30±0.56	51.76±9.84
	0.8	17.15±6.14	16.62±2.29	66.20±5.60
CNE2	0	52.66±2.62	26.94±3.06	20.41±0.43
	0.1	29.10±3.88	23.77±5.63	47.13±9.50
	0.2	11.74±6.57	15.89±8.75	72.37±2.18

± 21.09 mm^3 (Day 0) to 1209.06 ± 226.20 mm^3 (Day 30) with an increased rate of 775.4%. AP-3 given at a low dose of 0.3 mg/kg resulted in an inhibitory rate of 56.75% in tumor growth, with bodyweights having a slight decrease **(Figure 7).**

The Development of AP-3-peptide conjugates for EBV (+) NPC treatments

AP-3 at the low dose of 0.3 mg/kg could partly suppress NPC C666-1 tumor growth. In our previous study, we treated nude mice carrying gastric tumors with a slight higher dose of 0.5 mg/kg. We found AP-3 could significantly suppress tumor growth, but mouse bodyweights sharply dropped, with a mouse died [13]. We reduced the dose to 0.1 mg/kg, the bodyweights came back to normal, but AP-3 lost its anti-tumor efficacy at this lower dose. We demonstrated that AP-3 had super cytotoxic activity, but having severe side effects. AP-3 has a very narrow drug window and a less chance to be an anti-cancer drug alone. Thus, based on these findings, we have set out to modify AP-3 and link the AP-3 analog with peptide somatostatin or anti-SSTR2 mAb. The preliminary data showed that our drug conjugates could potently

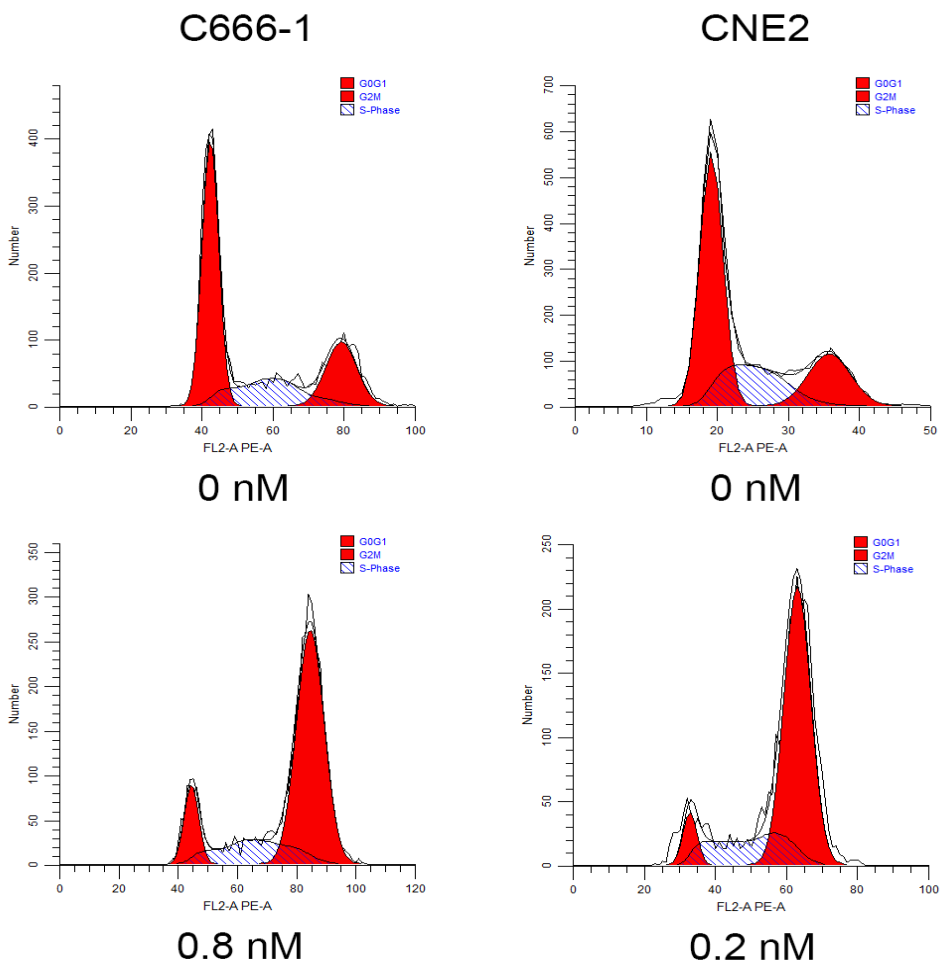

Figure 6 The potent compound AP-3 induced cell cycle arrest at G2/M Phases in EBV (+) NPC C666-1 and EBV (-) NPC CNE2 cells.

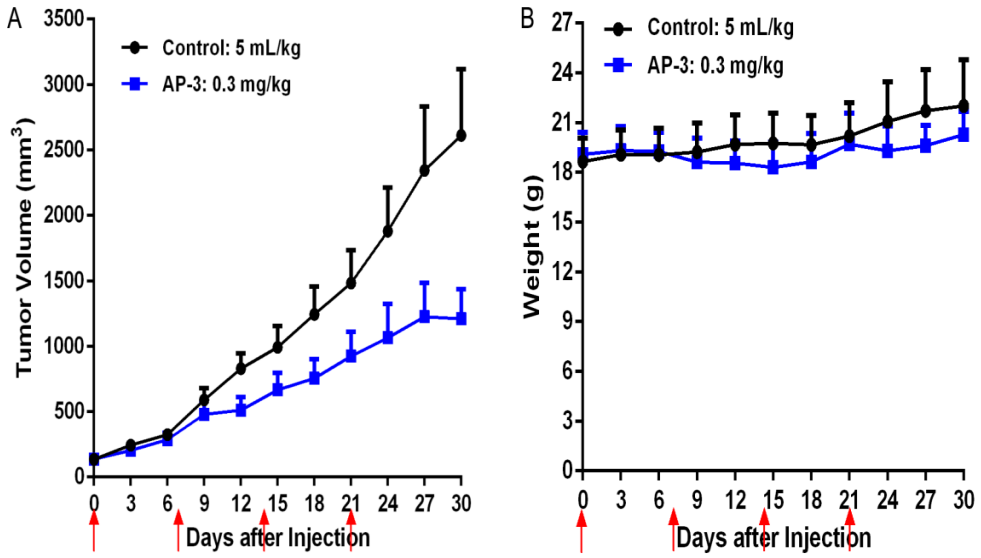

Figure 7 The suppressive effect of the compound AP-3 on EBV (+) NPC C666-1 tumor growth in nude mice. AP-3 was administrated by tail vein injection at a dose of 0.3 mg/kg and with a frequency of once a week for total four weeks. At day 0, tumor sizes were 135.30 ± 18.58 mm^3 in control group and 138.11 ± 21.09 mm^3 in AP-3 group, with 2611.35 ± 507.09 mm^3 in control group and 1209.06 ± 226.20 mm^3 in AP-3 group at day 30.

suppress tumor growth while retaining the cytotoxic activity of the AP-3 analog and the high binding affinity of SSTR2.

Discussion

Nasopharyngeal carcinoma (NPC) is highly chemo-sensitive and radio-sensitive [3,8]. Patients diagnosed with NPCs are usually at the late stage. They are generally treated with radio and chemotherapy. However, these patients frequently suffer from cancer recurrence. Further, given that the conventional chemotherapy generally causes severe side effects, new strategies have being developed to enhance the anti-cancer efficacy of these cytotoxic molecules in chemotherapy and meanwhile reduce their side effects [3,7,14]. Drug-targeting therapy is one of these new approaches [15,16]. For instance, one hot topic is to use monoclonal antibodies as drug delivery vehicles via conjugating these molecules to antibodies and form the so-called antibody-drug conjugates (ADCs) [17-19]. Due to their unique advantages, certain short synthetic peptides are also coupled with molecular drugs to form peptide-drug conjugates (PDCs) [15-20]. Most of these PDCs could deliver drugs to cancer cells via the interactions of ligands and receptors that are detected highly expressed in many cancer cells [15,21,22]. We also have successfully developed receptor-targeting PDCs. In our previous studies, these PDCs extremely enhanced the anti-tumor efficacy of the free drugs while greatly cut off the dose in use and accordingly reduce side effects. For example, JF-10-81 was a peptide-drug conjugate (PDC) via coupling the cytotoxic small molecule camptothecin to the N-terminus of somatostatin peptide, displayed its broad cytotoxic activities against tumor cell proliferation and tumor growth [15,23,24]. Particularly, radio-labeled somatostatin (named as Lutathera) had been successfully developed and approved by Food and Drug Administration (FDA) and applied for clinical treatments of SSTR-aberrant neuroblastoma [25-27].

NPC is strongly associated with EBV infection. In this study, our RNA-seq analysis showed that in the context of NPCs, the aberrant expression of SSTRs was strongly correlated with EBV infection. We also analzyed the expression of EBV genes in EBV (+) NPC C666-1 cells and detected abundant EBV transcripts **(Figure 2).** The expression of SSTR2 was also validated in C666-1 cells by qRT-PCR. We are also investigating the signaling networks among them and attempt to find the signaling pathway cascades.

In accordance with a recent report [12], we found that SSTR2 are highly expressed in EBV (+) NPC C666-1 cells, but undetectable in EBV (-) NPC CNE2 cells. We reasoned that the strategy to use a SSTR2-specific PDC and deliver drug to SSTR2-overexpressing NPC may be a viable option to manage EBV (+) NPC. We investigated the effects of the compounds **AP-3, camptothecin and** colchicine on NPC cell proliferation and tumor growth, and further evaluated the possibility of these compounds to be used for drug conjugates. The camptothecin conjugate JF-10-81 generated in our previous work [15,24] demonstrated its *in vitro* inhibitory activities of EBV-positive NPC cells growth (Data not shown). Here, AP-3 showed its more super inhibitory activities compared with the other two. Molecular structure analysis also showed that AP-3 could potentially serve as an anti-tumor warhead via linked to a drug delivery vehicle. Our preliminary data also demonstrated that the new AP-3 conjugates showed its more specificity and receptor-targeting compared to the free AP-3 (data not shown). The *in vivo* anti-tumor assays are under investigation.

Given that NPC recurrence frequently occurs after chemotherapy and radiotherapy, it is urgent to develop more effective therapeutic technologies or strategies. EBV is present in most of NPC cases and plays a critical role in carcinogenesis. Thus, EBV gene products and associated signaling molecules can serve as potential targets for precise treatment of this deadly disease through EBV-based immunotherapy and/or gene therapy [3,7]. The existence of EBV is also strongly associated with the aberrant expression of SSTR2 in EBV (+) NPC cells/tissues [12]. This also provides a new SSTR2-targeting therapeutics. In this study, we report that AP-3 has a good cytotoxic potency and serves as a good candidate for new drug conjugate. It may be a great perspective for the treatments of patients with advanced NPC in the future.

Acknowledgements

We would greatly acknowledge the supports from Shenzhen Science and Technology Program (Grant No: KQTD20170810154011370), Xiangtan Institute of Industrial Technology Collaborative Innovation, and Xiangtan Science and Technology.

References

1 Chou J, Lin YC, Kim J, You L, Xu Z, et al. (2008)Nasopharyngeal carcinoma--review of the molecular mechanisms of tumorigenesis. Head Neck 30: 946-963.

2 Yu MC, Yuan JM (2002) Epidemiology of nasopharyngeal carcinoma. Cancer Biology12: 421-429.

3 He JQ, Sun L, He J, Zhu C, Li P, et al. (2019) The Pathogenesis and Therapeutics of Nasopharyngeal Carcinoma. Health Sci J 13: 642.

4 Chua MLK, Wee JTS, Hui EP, Chan ATC (2016) Nasopharyngeal carcinoma. Lancet 387: 13.

5 Munz C(2019) Latency and lytic replication in Epstein-Barr virus-associated oncogenesis. Nat Rev Microbiol 17: 691-700.

6 Kheir F, Zhao M, Strong MJ, Yu Y, Nanbo A, et al. (2019) Detection of Epstein-Barr Virus Infection in Non-Small Cell Lung Cancer. Cancers (Basel) 11: 759.

7 Tao Q, Chan ATC (2007) Nasopharyngeal carcinoma: molecular pathogenesis and therapeutic developments. Expert Rev Mol Med 9: 1-24.

8 Ho CS (2017) Beating 'Guangdong cancer': a review and update on nasopharyngeal cancer. Hong Kong Med J 23: 497-502.

9 Zhang B, Cui B, Du J, Shen X, Wang K, et al. (2019) ATR activated

by EB virus facilitates chemotherapy resistance to cisplatin or 5-fluorouracil in human nasopharyngeal carcinoma. Cancer Manag Res 11: 573-585.

10 Strong MJ, Baddoo M, Nanbo A, Xu M, Puetter A, et al. (2014) Comprehensive high-throughput RNA sequencing analysis reveals contamination of multiple nasopharyngeal carcinoma cell lines with HeLa cell genomes. J Virol 88: 10696-10704.

11 Choi SJ, Jung SW, Huh S, Cho H, Kang H (2018) Phylogenetic comparison of Epstein-Barr virus genomes. J Microbiol 56: 525-533.

12 Lechner M, Schartinger VH, Steele CD, Nei WL, Ooft ML, et al. (2021) Somatostatin receptor 2 expression in nasopharyngeal cancer is induced by Epstein Barr virus infection: impact on prognosis, imaging and therapy. Nat Commun 12: 117.

13 Wang S, Ye J, Chen Y, Cui Z, ZhengQ, et al.(2021) The Potential Applications of the Potent Cytotoxic Ansamitocin P-3 in the Treatment of Gastric Carcinoma. Health Sci J 15: 828.

14 Korbi AE, Tkhayat SB, Bouatay R, Ferjaoui M, Kolsi N, et al. (2021) Therapeutic outcomes of nasopharyngeal carcinomas: a single-center study conducted at the Fattouma Bourguiba University Hospital in Monastir, Tunisia. Pan Afr Med J 38: 143.

15 Sun LC, Coy DH (2011)Somatostatin receptor-targeted anti-cancer therapy. Curr Drug Deliv 8: 2-10.

16 Yaghoubi S, Gharibi T, Karimi MH, Nezhad MS, Seifalian A, et al. (2021) Development and biological assessment of MMAE-trastuzumab antibody-drug conjugates (ADCs). Breast Cancer 28: 216-225.

17 Si Y, Xu Y, Guan J, Chen K, Kim S, et al. (2021) Anti-EGFR antibody-drug conjugate for triple-negative breast cancer therapy. Eng Life Sci 21: 37-44.

18 Bodyak ND, Mosher R, Yurkovetskiy AV, Yin M, Bu C, et al. (2021) The Dolaflexin-based antibody-drug conjugate XMT-1536 targets the solid tumor lineage antigen SLC34A2/NaPi2b. Mol Cancer Ther 20.

19 Hamilton JZ, Pires TA, Mitchell JA, Cochran JH, Emmerton KK, et al. (2021) Improving Antibody-Tubulysin Conjugates through Linker Chemistry and Site-Specific Conjugation. Chem Med Chem 16: 1077-1081.

20 Sun L, Coy DH(2016) Somatostatin and its Analogs. Curr Drug Targets 17: 529-537.

21 Jha A, Taïeb D, Carrasquillo JA, Pryma DA, Patel M, et al. (2021) High-Specific-Activity-(131)I-MIBG versus (177)Lu-DOTATATE Targeted Radionuclide Therapy for Metastatic Pheochromocytoma and Paraganglioma. Clin Cancer Res.

22 Shah RG, Merlin MA, Adant S, Zine-Eddine F, Beauregard JM, et al. (2021) Chemotherapy-Induced Upregulation of Somatostatin Receptor-2 Increases the Uptake and Efficacy of (177)Lu-DOTA-Octreotate in Neuroendocrine Tumor Cells. Cancers (Basel) 13: 232.

23 Sun LC, Luo J, Mackey LV, Fuselier JA, Coy DH, et al. (2007) A conjugate of camptothecin and a somatostatinanalog against prostate cancer cell invasion via a possible signaling pathway involving PI3K/Akt, alphaVbeta3/alphaVbeta5 and MMP-2/-9. Cancer Lett 246: 157-166.

24 Sun L, Morris LM, Luo J, Mackey LV, Leslie JS, et al. (2011) Application of human pancreatic carcinoid BON cells for receptor-targeted drug development. J Drug Target 19: 666-674.

25 Chin RI, Wu FS, Menda Y, Kim H (2021) Radiopharmaceuticals for Neuroendocrine Tumors. Semin Radiat Oncol 31: 60-70.

26 Underwood J, Sturchio G, Arnold S (2021) Patient Release and Instructions for Lutetium Dotatate Radiopharmaceutical Therapy. Health Phys.

27 Zahid A, Johnson DR, Kizilbash SH (2021) Efficacy of (177)Lu-Dotatate Therapy in the Treatment of Recurrent Meningioma. Mayo Clin ProcInnov Qual Outcomes 5: 236-240.